

Direct versus indirect optical recombination in Ge films grown on Si substratesG. Grzybowski,¹ R. Roucka,¹ J. Mathews,² L. Jiang,² R. T. Beeler,^{1,2} J. Kouvetakis,¹ and J. Menéndez^{2,*}¹*Department of Chemistry and Biochemistry, Arizona State University, Tempe, Arizona 85287-1604, USA*²*Department of Physics, Arizona State University, Tempe, Arizona 85287-1504, USA*

(Received 16 June 2011; revised manuscript received 21 July 2011; published 11 November 2011)

The optical emission spectra from Ge films on Si are markedly different from their bulk Ge counterparts. Whereas bulk Ge emission is dominated by the material's indirect gap, the photoluminescence signal from Ge films is mainly associated with its direct band gap. Using a new class of Ge-on-Si films grown by a recently introduced chemical vapor deposition approach, we study the direct and indirect photoluminescence from intrinsic and doped samples and we conclude that the origin of the discrepancy is the lack of self-absorption in thin Ge films combined with a deviation from quasi-equilibrium conditions in the conduction band of undoped films. The latter is confirmed by a simple model suggesting that the deviation from quasi-equilibrium is caused by the much shorter recombination lifetime in the films relative to bulk Ge.

DOI: [10.1103/PhysRevB.84.205307](https://doi.org/10.1103/PhysRevB.84.205307)

PACS number(s): 78.66.Db, 78.55.Ap, 81.15.Gh, 68.55.ag

I. INTRODUCTION

Germanium has unique optical properties related to the small separation of 0.14 eV between the absolute minimum of the conduction band at the *L*-point of the Brillouin zone and the Γ -point local minimum. Possible perturbation schemes leading to direct or quasi-direct band gap conditions have been known for a long time. These include *n*-type doping,¹ alloying with Sn² and the application of tensile strain.³ Over the past few years, these approaches have been contemplated as a possible way to integrate direct gap semiconductors with Si technology, fueling an intense research effort that culminated in the recent announcement of an optically pumped Ge-on-Si laser with emission close to 1550 nm.⁴

A remarkable feature of most published room temperature luminescence studies of Ge-on-Si films is the dominance of direct gap emission from the Γ -point local minimum in the conduction band to the absolute maximum of the valence band at the same $k = 0$ wave vector.^{5–12} This is in sharp contrast with similar experiments on bulk Ge samples,¹³ for which indirect gap emission from the *L*-minimum is much stronger. In this paper, we present a combined experimental and theoretical study focused on explaining this discrepancy. We argue that the difference between films and bulk arises from self-absorption effects, which are far more important in the bulk case, and—in the case of undoped films—from a deviation from quasi-equilibrium conditions in the presence of strong nonradiative recombination at the film–substrate interface. We present an explicit model that accounts for this effect. This peculiar behavior is the result of the unique properties of Ge, which has a direct gap slightly above the indirect edge and a carrier diffusion length of almost macroscopic dimensions.

II. EXPERIMENT

We study Sn-doped Ge-on-Si samples grown by a novel chemical vapor deposition approach introduced by Beeler *et al.*¹⁴ This method is an extrapolation—to ultralow Sn concentrations—of the growth procedure introduced by Bauer *et al.* to synthesize Ge_{1–y}Sn_y alloys.¹⁵ Briefly, the growth is conducted on high-resistivity Si(100) wafers via reactions of

digermane (Ge₂H₆) and deuterated stannane (SnD₄) diluted in H₂. Films with thicknesses up to several microns are commonly produced at high growth rates approaching 30 nm/min via reactions of Ge₂H₆ with appropriate amounts of SnD₄ at $T = 380$ – 400 °C. The incorporation of dopant levels of substitutional Sn into the Ge-on-Si films at nominal levels of 0.03%–0.15% is sufficient to suppress the traditional layer-plus-island growth mode (Stranski-Krastanov). The resultant layers are found to exhibit flat surfaces, relaxed strain states, and crystallinity/morphology comparable to those observed in the intrinsic materials, as evidenced by a range of analytical methods, including Rutherford backscattering, atomic force microscopy, high-resolution x-ray diffraction, secondary ion mass spectrometry, and cross-sectional transmission electron microscopy. The films can be systematically codoped with P and B atoms at controlled levels of up to 5×10^{19} cm^{–3} *in situ* using the single sources P(GeH₃)₃ and B₂H₆. This process produces tunable and highly controlled atomic profiles of the donor/acceptor atoms by judiciously adjusting the P(GeH₃)₃/Ge₂H₆ or B₂H₆/Ge₂H₆ ratio in the reaction mixture.

Photoluminescence (PL) is measured using a 980-nm laser focused to a ~ 100 - μ m spot on samples with thicknesses on the order of 1 μ m. The average incident power is 200 mW. The emitted light is analyzed with an $f = 320$ mm spectrometer equipped with a 600 lines/mm grating blazed at 2 μ m and collected with a single-channel, LN₂-cooled extended InGaAs detector that covers the 1.3- to 2.3- μ m range, well above and below the entire spectral range of Ge-like emission.

III. RESULTS AND DISCUSSION

Figure 1 shows the PL signal from a Sn-doped Ge film on Si. The as-grown sample shows no measurable PL, but after rapid thermal annealing (RTA) at 680 °C (which improves crystallinity, as seen from the narrowing of the x-ray diffraction peaks), followed by a heat treatment under hydrogen, as described in Ref. 8, the signal is maximized. The RTA treatment causes a tensile strain due to the thermal expansion mismatch with the Si substrate. In the sample in Fig. 1, we measured this strain by analyzing x-ray reciprocal space maps, and we obtained $\varepsilon = 0.24\%$. The main emission feature is

assigned to the direct gap E_0 . The shoulder at lower energies corresponds to indirect gap emission. The PL spectrum is virtually identical to that from a pure Ge film on Si (not shown) grown by the method introduced by Wistey *et al.* (Ref. 16). This confirms that the extremely small amount of Sn in the film does not change the optical properties in any measurable way. Accordingly, we simply refer to our films as Ge-on-Si, ignoring the small residual Sn concentration.

It seems natural to compare the film PL with bulk Ge emission. However, this comparison must be done with care because the PL spectrum from bulk Ge is severely distorted by self-absorption effects. With an ambipolar diffusion constant of $D = 65 \text{ cm}^2 \text{ s}^{-1}$ (Ref. 17) and a recombination lifetime of $\tau = 30 \text{ } \mu\text{s}$ (Ref. 18), the diffusion length of electron-hole pairs in Ge exceeds 0.4 mm and thus reabsorption cannot be neglected. Since the absorption coefficient is higher for 0.8-eV than for 0.7-eV photons, the observed direct gap PL is preferentially suppressed. By performing experiments on thin specimens in a transmission geometry with lamp illumination, for which reabsorption can be easily computed, Haynes¹⁹ generated a “corrected” emission spectrum for bulk Ge, which is shown as crosses in Fig. 1. This corrected spectrum shows clear peaks corresponding to direct and indirect transitions, with the direct gap emission being the strongest one. Since our Ge-on-Si films have thicknesses on the order of 1 μm , self-absorption corrections are much less important and the corresponding spectra should be compared with the “corrected” one from bulk Ge. Thus, the dominance of the direct gap emission in our Ge films is to be expected.

To understand the spectral lineshape and relative shifts, we model the direct gap emission using a generalized van Roosbroeck–Shockley expression, according to which the emission rate at photon energy E (in units of $\text{s}^{-1} \text{ cm}^{-3} \text{ eV}^{-1}$) is given by²⁰

$$R(E) = \left(\frac{n^2 E^2}{\pi^2 \hbar^3 c^2} \right) \alpha(E) \frac{1}{\exp \left[\frac{E - (E_{Fc} - E_{Fv})}{k_B T} \right] - 1}. \quad (1)$$

Here, n is the index of refraction, E_{Fc} (E_{Fv}) is the quasi-Fermi level for the conduction (valence) bands, and

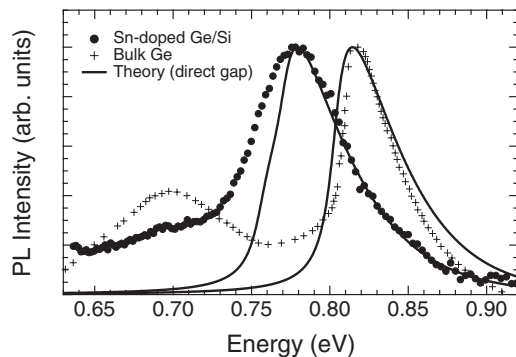


FIG. 1. Room temperature PL spectrum of a Ge-on-Si film compared with the corresponding spectrum from bulk Ge after self-absorption corrections (Ref. 17). The maximum is assigned to the direct gap emission. The weaker feature at lower energy corresponds to the indirect gap emission. The spectra are normalized to the same peak intensity. The solid lines are theoretical fits to the direct gap emission, as discussed in the text.

$\alpha(E)$ is the absorption coefficient at temperature T . The absorption can be written as $\alpha(E) = \alpha_0(E)[f_v(E) - f_c(E)]$, where $\alpha_0(E)$ is the absorption coefficient for empty conduction bands and full valence bands. This factorization is valid for parabolic bands, for which the Fermi functions $f_v(E) = 1/[1 + \exp[(E_v(E) - E_{Fv})/k_B T]]$ and $f_c(E) = 1/[1 + \exp[(E_c(E) - E_{Fc})/k_B T]]$ give the occupation probability for the valence band state of energy E_v and the conduction band state of energy E_c such that $E_c - E_v = E$. In all of these expressions, we use the standard notation for fundamental physical constants. For the function $\alpha_0(E)$, we developed an analytical model, discussed in full detail in the appendix of Ref. 21, which reproduces the experimental absorption curve over a range of up to 0.1 eV above the direct band gap based on standard band structure parameters, without introducing any additional parameter to adjust for the absorption strength. As explained in Ref. 21, including excitonic effects is critical to obtain this agreement. The advantage of using a realistic analytical absorption model—as opposed to the experimental absorption coefficient—is that the effect of temperature and strain can be easily introduced. For the temperature T dependence of the Ge direct band gap, we use an expression of the form $E_0 = E_0(0) - \alpha T^2/(T + \beta)$, with $E_0(0) = 0.891 \text{ eV}$, $\alpha = 5.82 \times 10^{-4} \text{ eV/K}$, and $\beta = 296 \text{ K}$, which reproduces well the literature data and our measurements of the direct band gap. For the strain calculations, we use the deformation potentials given in Ref. 21. While the calculated absorption is limited to the direct band gap only, the conduction band minima at the L -points are fully taken into account for the computation of E_{Fc} . The density of states for the L -valley is computed using a longitudinal effective mass $m_l = 1.58m_0$ (Ref. 22) where m_0 is the electron’s free mass. A transverse effective mass m_t is obtained from a standard $\mathbf{k} \cdot \mathbf{p}$ expression with a momentum matrix element $P = 12.6 \text{ eV}$, which gives $m_t = 0.080m_0$ for pure Ge at 300K. The calculated relative populations n_Γ/n_L of the two conduction band valleys, which are important for the subsequent discussion, are shown in Fig. 2 as a function of the total electron population.

Calculated emission profiles using Eq. (1) are shown as solid lines in Fig. 1. For the bulk Ge case, we find a good agreement in peak position and overall lineshape, assuming

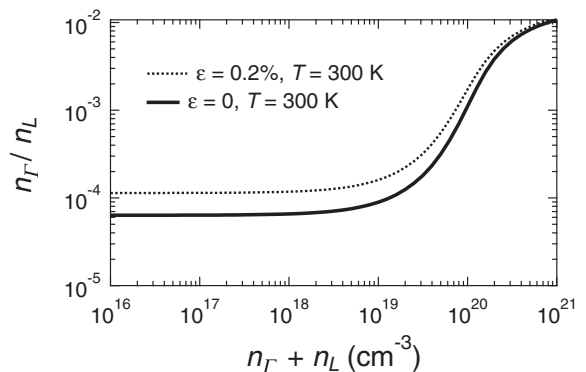


FIG. 2. Population ratio for the Γ - and L -valleys in the conduction band of Ge as a function of the total electron density in the conduction band. The calculations are shown for relaxed Ge ($\varepsilon = 0$), as well as for Ge with a biaxial tensile strain in the (001) plane ($\varepsilon = 0.2\%$).

that the sample temperature is $T = 290\text{K}$ and the photoexcited electron density is less than $1 \times 10^{18} \text{ cm}^{-3}$. The residual disagreement between theory and experiment may be due to systematic errors in the self-absorption correction, caused mainly by the absorption coefficient of Ge in this spectral range depending strongly on temperature.²³ For the Ge-on-Si sample, the emission is calculated using the measured tensile strain of 0.24% and a sample temperature of 320 K. The tensile strain explains 80% of the redshift with respect to bulk Ge, whereas the higher sample temperature, which is expected for laser excitation, accounts the remaining 20%.

Most prior experimental work on light emission from Ge-on-Si films is based on standard Ge or InGaAs detectors with excellent noise-equivalent power characteristics but with cutoffs near 0.7 eV, which make it difficult to measure indirect gap PL. However, researchers using extended range detectors comparable to ours have noticed an enhancement of the intensity ratio $I_{\text{dir}}/I_{\text{ind}}$ between direct and indirect emission in Ge-on-Si films relative to bulk Ge uncorrected for self-absorption.^{11–13} Ge_{1–y}Sn_y films on Si also show a similar trend.^{8,9} These relative intensity changes have been attributed to the presence of defects, but our preceding analysis indicates that the self-absorption correction removes—at least in part—the discrepancy between bulk and thin-film Ge. Moreover, any model that invokes defects must provide a mechanism by which the population ratio n_{Γ}/n_L changes, since this ratio determines the relative intensity $I_{\text{dir}}/I_{\text{ind}}$.²⁴ This is far from obvious. If quasi-equilibrium conditions prevail in the conduction band, i.e., if there is a common conduction band quasi-Fermi level E_{Fc} , the n_{Γ}/n_L ratio depends only on the temperature, the energy separation between the two valleys, and their corresponding density of states. The enhancement of nonradiative recombination via defects reduces the steady-state photoexcitation level $n_{\Gamma} + n_L$, but, as seen in Fig. 2, the ratio n_{Γ}/n_L is insensitive to $n_{\Gamma} + n_L$ up to levels close to $1 \times 10^{19} \text{ cm}^{-3}$, much higher than can be achieved by photoexcitation. Moreover, from Fig. 2, it is apparent that a decrease in $n_{\Gamma} + n_L$ would lead to a decrease in n_{Γ}/n_L and thus to a decrease, not an increase, in $I_{\text{dir}}/I_{\text{ind}}$. We might also expect a decrease in $I_{\text{dir}}/I_{\text{ind}}$ if defects relax the crystal momentum conservation rules and enhance the no-phonon indirect recombination. Jan *et al.* argued that the presence of defects lead to a spread of trap levels in momentum space that enhances the nonradiative recombination from the indirect edge,¹¹ but it is not obvious how $I_{\text{dir}}/I_{\text{ind}}$ might change if quasi-equilibrium is preserved. It appears that any model based on defects should involve a change in the density of states (which would require exceptionally high defect densities) or a deviation from quasi-equilibrium conditions.

If defects do not play an important role in determining the relative intensities of direct and indirect emission, we should be able to explain the $I_{\text{dir}}/I_{\text{ind}}$ ratios in Fig. 1 based on the valley population ratios in Fig. 2. We obtain approximate values for $I_{\text{dir}}/I_{\text{ind}}$ by fitting the data with simple empirical expressions that appear in commercial data analysis packages. For the direct emission we use exponentially modified Gaussians,²⁵ which fit the theoretical profiles in Fig. 1 remarkably well, and for the indirect emission we use a simple Gaussian. The width of the Gaussian is fit to the bulk data of Haynes¹⁹ and kept fixed

for subsequent fits of all samples, a reasonable assumption because the width of the indirect gap emission is essentially given by phonon energies that are expected to change little in Ge films relative to bulk Ge. Under these conditions, using the peak areas, we obtain $I_{\text{dir}}/I_{\text{ind}} \approx 1.3 \pm 0.2$ for bulk Ge and $I_{\text{dir}}/I_{\text{ind}} = 7 \pm 2$ for the Ge-on-Si film in Fig. 1, the large errors arising from the different results obtained by assuming alternative expressions for the spectral background. The higher sample temperature and tensile strain in the Ge-on-Si sample enhances its n_{Γ}/n_L ratio with respect to the bulk sample, as seen in Fig. 2. We compute a theoretical enhancement factor of 2.9, which is less than the experimental enhancement $7/1.3 = 5.4$. This suggests that an additional contribution may be needed to explain the high $I_{\text{dir}}/I_{\text{ind}}$ ratio in the Ge-on-Si sample.

To investigate the $I_{\text{dir}}/I_{\text{ind}}$ ratio in more detail, we carried out PL experiments in doped n -type Ge films. The rationale behind these experiments is that for doping levels close to 10^{19} cm^{-3} , the n_{Γ}/n_L population ratio should be determined by standard equilibrium conditions between the two valleys, not by the photoexcitation process. Therefore, if photoexcited *intrinsic* films somehow deviate from quasi-equilibrium, their doped counterparts should exhibit quite different $I_{\text{dir}}/I_{\text{ind}}$ ratios. The experimental result is shown as solid circles in Fig. 3 for a 1200-nm-thick Ge-on-Si film with a doping concentration of $1.9 \times 10^{19} \text{ cm}^{-3}$ and vanishing $\varepsilon = 0.05\%$. This low level of strain is possible because the RTA step can be omitted due to the PL enhancement associated with doping. Quite remarkably, the PL spectrum lineshape now looks more similar to the emission from bulk Ge, which is also reproduced for convenience in Fig. 3. Despite the vanishing strain, there is still a significant shift between the two spectra, which can be explained in terms of band gap renormalization induced by doping. This is discussed in detail in Sec. V. It does not affect the analysis in this section, because doping shifts the conduction band rigidly.²⁶ The $I_{\text{dir}}/I_{\text{ind}}$ for the doped Ge-on-Si sample is 1.7 ± 0.3 , clearly much less than the ratio $I_{\text{dir}}/I_{\text{ind}} = 7 \pm 2$ observed in Fig. 1, even though a calculation based on Fig. 2 predicts that the difference between the two ratios should not exceed 25%. Next, the sample is RTA treated to

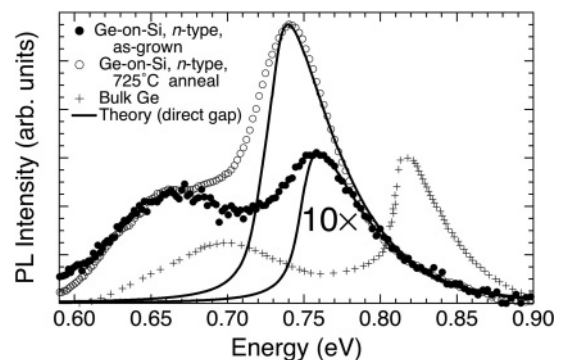


FIG. 3. Room temperature PL spectrum of a fully relaxed, n -type Ge-on-Si film with a thickness of 1200 nm and carrier density of $\sim 1.9 \times 10^{19} \text{ cm}^{-3}$, as grown (solid circles) and annealed at 725 °C (empty circles). Bulk Ge emission from Haynes (Ref. 19) is shown as crosses. The solid lines are fits with Eq. (1). The bulk Ge spectrum has been normalized to the same maximum intensity as that from the as-grown Ge-on-Si sample.

725 °C; its postannealing PL spectrum is shown as empty circles in Fig. 3. The overall intensity increases by a factor of 20, which correlates with a large reduction in the full width at half maximum of the x-ray diffraction peak, from 0.48° (as grown) to 0.061° (725 °C). This suggests that the improved PL is due to a reduced nonradiative recombination rate and explains the failure to observe PL in undoped, unannealed samples. On the other hand, the $I_{\text{dir}}/I_{\text{ind}}$ ratio only increases by 50% to 2.6 ± 0.3 after annealing. This can be explained in terms of the 0.18% tensile strain induced by the annealing process, which leads to a predicted increase of 45% in the n_{Γ}/n_L ratio, in good agreement with the experimental results.

The conclusion from the preceding experiments is that the results from doped Ge-on-Si films can be understood in terms of quasi-equilibrium conditions in the conduction band. Consistent with this model, the elimination of defects via annealing changes the overall intensity dramatically, but the $I_{\text{dir}}/I_{\text{ind}}$ ratio only changes according to the quasi-equilibrium model following the strain induced by the annealing process. On the other hand, the $I_{\text{dir}}/I_{\text{ind}}$ ratio in intrinsic, undoped Ge-on-Si films is too large compared with bulk Ge and with doped Ge-on-Si films, suggesting that in this case an additional mechanism affects this ratio. As mentioned previously, the presence of defects can only be invoked if a mechanism can be identified that generates a departure from quasi-equilibrium in the conduction band. A model that meets this requirement is discussed in the next section.

IV. NONEQUILIBRIUM MODEL

The foregoing discussion suggests that quasi-equilibrium conditions may not prevail in the conduction band of photoexcited intrinsic Ge-on-Si films. We present here a simple model that provides a mechanism for the departure from equilibrium. We consider a system of two interacting states, representing the Γ - and L -valleys. We assume that electrons are being pumped into the Γ -valley at a rate of G electrons/s. This is the case in Ge under 980-nm laser excitation. The excited electrons redistribute themselves between the two valleys, and they recombine with holes via radiative and nonradiative channels. The simplest rate equations that can be written to represent this situation are

$$\begin{aligned} \frac{dn_{\Gamma}}{dt} &= G - \left(\frac{1}{\tau_{\Gamma L}} + \frac{1}{\tau_{\Gamma}} \right) n_{\Gamma} + \frac{1}{\tau_{L\Gamma}} n_L \\ \frac{dn_L}{dt} &= - \left(\frac{1}{\tau_{L\Gamma}} + \frac{1}{\tau_L} \right) n_L + \frac{1}{\tau_{\Gamma L}} n_{\Gamma} \end{aligned} \quad (2)$$

The transfer rates between the valleys are characterized by the time constants $\tau_{\Gamma L}$ and $\tau_{L\Gamma}$, and the constants τ_{Γ} and τ_L represent the recombination lifetimes for each valley. An additional coupled equation involves the valence band holes, but this equation is not needed for the argument we are about to make. Eq. (2) is a generalization of a two-state model introduced by Stanton and Bailey to discuss electron dynamics in GaAs and InP.²⁷ If the generation and recombination terms are deleted, the system of equations has asymptotic solutions for $t \rightarrow \infty$ that imply $n_{\Gamma}(\infty)/n_L(\infty) = \tau_{\Gamma L}/\tau_{L\Gamma}$ for arbitrary initial occupations.²⁷ Since this limit corresponds to quasi-equilibrium, the $\tau_{\Gamma L}/\tau_{L\Gamma}$ ratio must equal the ratio n_{Γ}/n_L

computed in Fig. 2, which leads to $\tau_{\Gamma L}/\tau_{L\Gamma} \leq 10^{-4}$ for the total electron concentrations of relevance for this discussion. If we now consider the full Eq. (2), the time derivatives become zero when steady-state conditions are reached (e.g. under illumination with a continuous-wave laser). We then obtain

$$\frac{n_{\Gamma}}{n_L} = \frac{\tau_{\Gamma L}}{\tau_{L\Gamma}} + \frac{\tau_{\Gamma L}}{\tau_L}. \quad (3)$$

Therefore, we can expect deviations from equilibrium if the second term on the right-hand side of Eq. (3) is comparable to or greater than 10^{-4} . Under such circumstances, the relative valley populations cannot be computed using a common quasi-Fermi level. The transfer rate $\tau_{\Gamma L}$ in Ge has been measured by time-resolved inelastic light scattering, and its value is $\tau_{\Gamma L} = 1.2$ ps.²⁸ On the other hand, the recombination time τ_L can be associated with the minority carrier lifetime, which in bulk Ge is ~ 30 μ s.¹⁸ Thus, for bulk Ge, $\tau_{\Gamma L}/\tau_L$ is 4×10^{-8} , and the second term in Eq. (3) is much smaller than the first term. In other words, deviations from quasi-thermal equilibrium in bulk Ge are negligible, and the PL spectrum can be calculated by assuming a unique quasi-Fermi level for the conduction band.

The situation is very different in Ge-on-Si materials due to the presence of a surface and an interface. The recombination velocity s at a bare Ge surface is ~ 140 cm/s.²⁹ On the other hand, the interface recombination velocity at a dislocated Si-Ge interface can be as high as $s = 4000$ cm/s.³⁰ Using this value for a film thickness $W = 1$ μ m, the effective lifetime becomes $\tau_L = W/2s = 12$ ns so that $\tau_{\Gamma L}/\tau_L = 10^{-4}$, and the second term on the right-hand side of Eq. (3) is no longer negligible. For this particular value of $\tau_{\Gamma L}/\tau_L$, the ratio n_{Γ}/n_L would be doubled relative to the quasi-equilibrium prediction, and the $I_{\text{dir}}/I_{\text{ind}}$ PL ratio would be enhanced proportionally. (Both n_{Γ} and n_L decrease in absolute terms for shorter recombination lifetimes, so the overall PL intensity is reduced, as observed experimentally). Interestingly, from studies of $\text{Ge}_{1-y}\text{Sn}_y$ devices with a thickness $W = 300$ nm, we find recombination lifetimes approaching 5 ns,³¹ close to our estimates based on interface recombination velocities. In Fig. 4, we show PL spectra from three p -type samples. These samples have comparable total thicknesses but different doping profiles. Sample A is highly doped ($p = 1 \times 10^{19}$ cm⁻³), whereas sample B has much lower doping ($p = 1 \times 10^{18}$ cm⁻³). The integrated PL intensity of sample B is six times weaker than that of sample A, in reasonable agreement with the doping concentrations. Sample C is a backsurface-field (BSF) type of structure, in which the bottom half of the Ge layer is highly doped ($p = 1 \times 10^{19}$ cm⁻³) and the top half is very lightly doped ($p = 1 \times 10^{17}$ cm⁻³). Accordingly, emission from the top layer should be much weaker than that of sample B, and emission from the bottom layer should be significantly weaker than that of sample A because this layer is thinner and it is located ~ 500 nm below the surface. However, PL from sample C is strong, and the peak energy is higher than that of sample A. This suggests that most of the emission originates from the top layer, where band gap renormalization due to doping should be negligible. We associate this higher-than-expected emission from the top layer to the built-in potential in the BSF structure, which repels the photoexcited electrons in the lightly doped layer away from the Si interface. This behavior is consistent with the preceding suggestion that defects at the

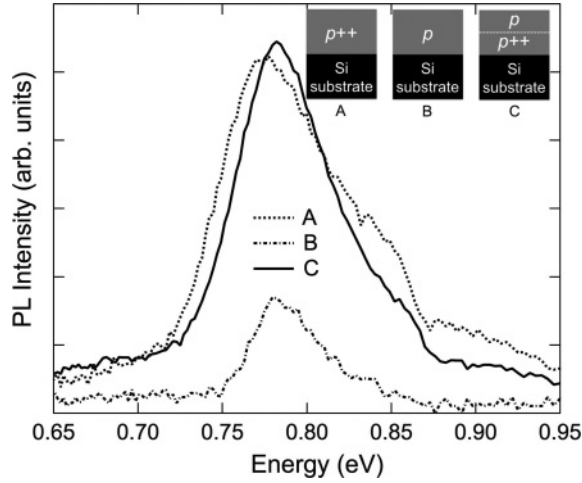


FIG. 4. Room temperature PL intensity from p -type Ge-on-Si samples. Doping concentrations are $p^{++} = 1 \times 10^{19} \text{ cm}^{-3}$ (samples A and C), $p = 1 \times 10^{18} \text{ cm}^{-3}$ (sample B), and $p = 1 \times 10^{17} \text{ cm}^{-3}$ (sample C). Thicknesses are 830 nm (sample A), 730 nm (sample B), and 960 nm (sample C). In sample C, the p^{++} and p layers have equal thickness. All samples were subjected to three cycles of postgrowth RTA at 680°C (10 s each).

Si interface are the main cause of nonradiative recombination in these structures.

The $I_{\text{dir}}/I_{\text{ind}}$ ratios in the p -doped samples are very high, to the point that the indirect gap signal is difficult to quantify. This is qualitatively consistent with the preceding analysis, since only in n -type samples would we expect ratios approaching the equilibrium conditions depicted in Fig. 2. However, a quantitative comparison of $I_{\text{dir}}/I_{\text{ind}}$ ratios between n -type and p -type Ge-on-Si layers may not be straightforward, since even in highly doped p -type bulk Ge Wagner and Viña observed a laser wavelength dependence of the $I_{\text{dir}}/I_{\text{ind}}$ ratios.³² In the Wagner-Viña experiment, these ratios were found to increase as the electrons become preferentially pumped into the Γ -valley, the situation mimicked by Eq. (2). Thus, our simple model may explain the experimental observations not only in Ge-on-Si materials but also on very highly doped p -type bulk material. In this latter case, there are no interfaces with high recombination rates, so the dominant nonradiative recombination mechanism should be associated with defects induced by the heavy doping.

V. BAND GAP RENORMALIZATION

As briefly hinted at earlier, we might expect the emission maximum of the as-grown doped Ge-on-Si film in Fig. 3 (dark circles) to be much closer to that of bulk Ge than the PL maximum of the intrinsic, tensile-strained quasi-Ge sample in Fig. 1. Surprisingly, the opposite is true. The emission maximum in the doped quasi-Ge sample is located at 0.755 eV, whereas the emission maximum for the intrinsic quasi-Ge sample in Fig. 1 appears at 0.778 eV. A possible explanation is that the presence of dopant atoms shifts the absorption edges in Ge, as has been shown in absorption measurements, where a clear redshift is detected.²⁶ Recent PL work on phosphorus-doped Ge also shows a redshift as a function of the P concentration, although its quantification is difficult

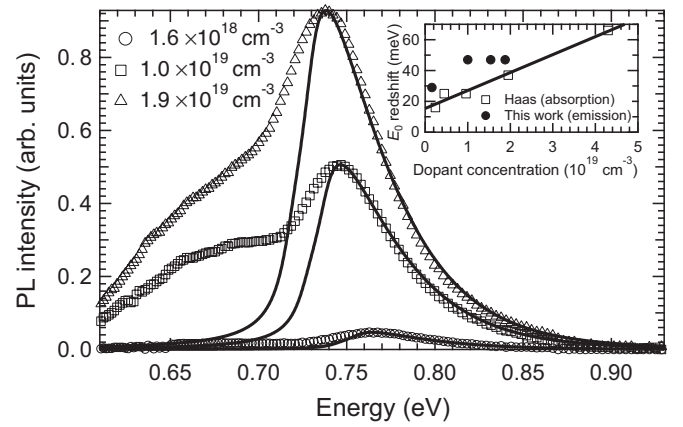


FIG. 5. Room temperature PL spectrum from Ge-on-Si films with different P doping concentrations. The solid lines are theoretical fits to the direct gap emission. The inset shows the redshift needed to adjust the spectra, compared with absorption measurements of the direct gap renormalization induced by P impurities in Ge (Ref. 10).

because the PL maximum is near the cutoff wavelength of the detector used by these researchers.³³ On the other hand, PL experiments using doped Ge-on-Si films show no such shift.⁵ The redshift we observe cannot be explained in terms of poor crystallinity, since the peak shifts further to lower energies upon annealing, as seen in Fig. 3 (white circles). To quantify this effect, we simply allow for an adjustable rigid energy shift of the absorption coefficient. The fit redshifts are then 40 meV for the doped, as-grown sample in Fig. 3 and 47 meV for the same sample annealed at 725°C . These are close to the redshift of 37 meV in the direct gap absorption observed by Haas for a P-doped Ge sample at a level of $1.95 \times 10^{19} \text{ cm}^{-3}$.²⁶ To confirm this correlation, we carried out additional PL experiments in samples with different doping levels. The results are shown in Fig. 5. The overall intensity and the $I_{\text{dir}}/I_{\text{ind}}$ ratio increase as a function of the doping concentration, as expected from our models and reported earlier.⁵ In the inset, we compare the shifts measured by Haas²⁶ with the shifts determined from our fits. They seem to follow a similar trend, with the emission shifts higher by ~ 10 meV relative to the absorption shifts, which may reflect a systematic error associated with the two methods of band gap determination. We believe that these results provide a strong indication that the redshifts observed in our samples are caused by the dopant atoms and that the same mechanism is responsible for the shift in emission and absorption energies.

Band gap renormalization effects are not limited to the band minima where the donor electrons happen to reside. The shifts are caused by the perturbation associated with the presence of foreign atoms,³⁴ which changes the entire band structure. In Haas' absorption experiments, the indirect edge is seen to redshift by the same amount as the direct edge.²⁶ This is a nontrivial result which implies that the n_{Γ}/n_L ratio is not affected by renormalization effects, justifying our preceding comparison of $I_{\text{dir}}/I_{\text{ind}}$ ratios in doped and undoped samples. In the PL experiments, however, the separation between direct and indirect maxima decreases from 118 meV in the bulk case to 99 meV in the doped quasi-Ge sample. We do not think this

is inconsistent with a rigid shift of the two edges because the lineshape of the indirect gap emission may be affected by the presence of impurities.

VI. CONCLUSION

The new experimental data presented here and the associated analysis indicate that the dominance of direct gap emission in Ge-on-Si films is due to two effects. In all Ge-on-Si thin films, the lack of significant self-absorption effects enhances the relative intensity of the direct gap emission in the experimental spectra. In *n*-doped Ge-on-Si films, we find no evidence for any other contribution to the enhancement of direct gap emission. In intrinsic or *p*-type Ge-on-Si films, where the electron population in the conduction band is produced by photoexcitation, there appears to be an additional

enhancement of the direct gap emission relative to the indirect gap emission that suggests a departure from quasi-equilibrium conditions. A model is proposed to account for this departure in terms of a much shorter recombination lifetime than in bulk Ge. The $I_{\text{dir}}/I_{\text{ind}}$ ratio in intrinsic and *p*-type materials then becomes a useful figure of merit to assess the quality of the material for possible laser applications.

ACKNOWLEDGMENTS

This work was supported by the US Air Force under Department of Defense Air Force Office of Scientific Research Contract No. FA9550-06-01-0442 (Multidisciplinary University Research Initiative program) and by the National Science Foundation under Grant No. DMR-0907600.

*jose.menendez@asu.edu

- ¹M. J. Adams and P. T. Landsberg, in *9th International Conference on the Physics of Semiconductors* (Akademiya Nauk, Moscow, 1968), p. 619.
- ²D. W. Jenkins and J. D. Dow, *Phys. Rev. B* **36**, 7994 (1987).
- ³R. A. Soref and L. Friedman, *Superlattice. Microstruct.* **14**, 189 (1993).
- ⁴J. Liu, X. Sun, R. Camacho-Aguilera, L. C. Kimerling, and J. Michel, *Opt. Lett.* **35**, 679 (2010).
- ⁵X. Sun, J. Liu, L. C. Kimerling, and J. Michel, *Appl. Phys. Lett.* **95**, 011911 (2009).
- ⁶S.-L. Cheng, J. Lu, G. Shambat, H.-Y. Yu, K. Saraswat, J. Vuckovic, and Y. Nishi, *Opt. Express* **17**, 10019 (2009).
- ⁷X. Sun, J. Liu, L. C. Kimerling, and J. Michel, *Opt. Lett.* **34**, 1198 (2009).
- ⁸J. Mathews, R. T. Beeler, J. Tolle, C. Xu, R. Roucka, J. Kouvetakis, and J. Menéndez, *Appl. Phys. Lett.* **97**, 221912 (2010).
- ⁹R. Roucka, J. Mathews, R. T. Beeler, J. Tolle, J. Kouvetakis, and J. Menéndez, *Appl. Phys. Lett.* **98**, 061109 (2011).
- ¹⁰S.-L. Cheng, G. Shambat, J. Lu, H.-Y. Yu, K. Saraswat, T. I. Kamins, J. Vuckovic, and Y. Nishi, *Appl. Phys. Lett.* **98**, 211101 (2011).
- ¹¹S. R. Jan, C. Y. Chen, C. H. Lee, S. T. Chan, K. L. Peng, C. W. Liu, Y. Yamamoto, and B. Tillack, *Appl. Phys. Lett.* **98**, 141105 (2011).
- ¹²M. Kittler, T. Arguirov, M. Oehme, Y. Yamamoto, B. Tillack, and N. V. Abrosimov, *Phys. Status Solidi A* **208**, 754 (2011).
- ¹³T. H. Cheng, C. Y. Ko, C. Y. Chen, K. L. Peng, G. L. Luo, C. W. Liu, and H. H. Tseng, *Appl. Phys. Lett.* **96**, 091105 (2010).
- ¹⁴R. T. Beeler, G. Grzybowski, R. Roucka, L. Jiang, J. Mathews, D. J. Smith, J. Menéndez, and J. Kouvetakis, *Chem. Mater.* **23**, 4480 (2011).
- ¹⁵M. Bauer, J. Taraci, J. Tolle, A. V. G. Chizmeshya, S. Zollner, D. J. Smith, J. Menéndez, C. Hu, and J. Kouvetakis, *Appl. Phys. Lett.* **81**, 2992 (2002).

- ¹⁶M. A. Wistey, Y. Y. Fang, J. Tolle, A. V. G. Chizmeshya, and J. Kouvetakis, *Appl. Phys. Lett.* **90**, 082108 (2007).
- ¹⁷A. L. Smirl, S. C. Moss, and J. R. Lindle, *Phys. Rev. B* **25**, 2645 (1982).
- ¹⁸E. Gaubas and J. Vanhellemont, *Appl. Phys. Lett.* **89**, 142106 (2006).
- ¹⁹J. R. Haynes, *Phys. Rev.* **98**, 1866 (1955).
- ²⁰S. L. Chuang, *Physics of Optoelectronic Devices* (Wiley, New York, 1995).
- ²¹R. Roucka, R. Beeler, J. Mathews, M.-Y. Ryu, Y. Kee Yeo, J. Menéndez, and J. Kouvetakis, *J. Appl. Phys.* **109**, 103115 (2011).
- ²²O. Madelung ed., *Semiconductors: Intrinsic Properties of Group IV Elements and III-V, II-VI, and I-VII Compounds* (Springer-Verlag, Berlin, 1985).
- ²³V. Sorianello, A. Perna, L. Colace, G. Assanto, H. C. Luan, and L. C. Kimerling, *Appl. Phys. Lett.* **93**, 111115 (2008).
- ²⁴W. Klingenstein and H. Schweizer, *Solid-State Electron.* **21**, 1371.
- ²⁵E. Grushka, *Anal. Chem.* **44**, 1733 (1972).
- ²⁶C. Haas, *Phys. Rev.* **125**, 1965 (1962).
- ²⁷C. J. Stanton and D. W. Bailey, *Phys. Rev. B* **45**, 8369 (1992).
- ²⁸K. Tanaka, H. Ohtake, and T. Suemoto, *Phys. Rev. Lett.* **71**, 1935 (1993).
- ²⁹B. P. Swain, H. Takato, Z. Liu, and I. Sakata, *Sol. Energ. Mater. Sol. Cell.* **95**, 84 (2011).
- ³⁰A. Trita, I. Cristiani, V. Degiorgio, D. Chrastina, and H. von Känel, *Appl. Phys. Lett.* **91**, 041112 (2007).
- ³¹J. Mathews, Ph.D. Thesis, Arizona State University, US, 2011.
- ³²J. Wagner and L. Viña, *Phys. Rev. B* **30**, 7030 (1984).
- ³³M. El Kurdi, T. Kociniowski, T. P. Ngo, J. Boulmer, D. Débarre, P. Boucaud, J. F. Damlencourt, O. Kermarrec, and D. Bensahel, *Appl. Phys. Lett.* **94**, 191107 (2009).
- ³⁴P. B. Allen, *Phys. Rev. B* **18**, 5217 (1978).